JTTEE5 23:213–219
DOI: 10.1007/s11666-013-0004-y
1059-9630/$19.00 © ASM International

Plasma Spray Physical Vapor Deposition of $La_{1-x}Sr_xCo_yFe_{1-y}O_{3-\delta}$ Thin-Film Oxygen Transport Membrane on Porous Metallic Supports

Maria Ophelia Jarligo, Georg Mauer, Martin Bram, Stefan Baumann, and Robert Vaßen

(Submitted May 26, 2013; in revised form August 17, 2013)

Plasma spray physical vapor deposition (PS-PVD) is a very promising route to manufacture ceramic coatings, combining the efficiency of thermal spray processes and characteristic features of thin PVD coatings. Recently, this technique has been investigated to effectively deposit dense thin films of perovskites particularly with the composition of $La_{0.58}Sr_{0.4}Co_{0.2}Fe_{0.8}O_{3-\delta}$ (LSCF) for application in gas separation membranes. Furthermore, asymmetric type of membranes with porous metallic supports has also attracted research attention due to the advantage of good mechanical properties suitable for use at high temperatures and high permeation rates. In this work, both approaches are combined to manufacture oxygen transport membranes made of gastight LSCF thin film by PS-PVD on porous NiCoCrAlY metallic supports. The deposition of homogenous dense thin film is challenged by the tendency of LSCF to decompose during thermal spray processes, irregular surface profile of the porous metallic substrate and crack and pore-formation in typical ceramic thermal spray coatings. Microstructure formation and coating build-up during PS-PVD as well as the annealing behavior at different temperatures of LSCF thin films were investigated. Finally, measurements of leak rates and oxygen permeation rates at elevated temperatures show promising results for the optimized membranes.

Keywords perovskite $La_{1-x}Sr_xCo_yFe_{1-y}O_{3-\delta}$, plasma spray physical vapor deposition, porous metallic support, oxygen transport membrane, thin films

1. Introduction

Plasma spray physical vapor deposition (PS-PVD) is a new processing technique that combines the economic and operational advantages of conventional atmospheric plasma spray (APS) and the high deposition efficiency of physical vapor deposition (PVD) techniques to create unique microstructures (Ref 1-3). Also known as very low pressure plasma spray (VLPPS) or low pressure plasma spray-thin film (LPPS-TF), PS-PVD operates in considerably low pressure, ranging from 50 to 200 Pa. With this condition, the resulting plasma can extend to more than 2-m long and 200-400 mm in diameter. The process produces supersonic gas streams about 2000 m/s with temperatures higher than 6000 °C (Ref 1). The distribution of temperature and particle velocity is more uniform, although the plasma is significantly larger compared to the standard vacuum plasma spray (VPS) techniques (Ref 4). The high power capability of the plasma torch ($<$150 kW) at pressures below 2 kPa, can result in the vaporization of the injected ceramic powder and deposition onto a target substrate. The vaporized material incorporated in the plasma stream provides some non-line-of-sight coverage, which is not achievable using PVD or other conventional plasma spray techniques (Ref 1). This technology has been reported to coat large and thin areas as well as surfaces with complex geometries for a very short time (~10 μm/m^2-min) (Ref 5). The process is therefore attractive for fabrication of homogeneous ceramic thin films such as oxygen transport membranes (OTM) in gas purification industries. These membranes are gastight and consist of mixed ionic-electronic conductors (MIEC) that allow oxygen diffusion through vacancies in the oxygen site of the crystal lattice. Based on bulk diffusion, dense and as thin as possible coatings are required to produce high oxygen permeation fluxes across a membrane with oxygen partial pressure gradient (Ref 6). Unlike wet chemical routes such as screen-printing and tape casting which are typically used to manufacture ceramic thin films, plasma spray does not require a subsequent sintering procedure to remove organic solvents incorporated in the coating precursors. Previous works have already reported successful deposition of thin and dense coatings using PS-PVD (Ref 1, 2, 7, 8).

This article is an invited paper selected from presentations at the 2013 International Thermal Spray Conference, held May 13-15, 2013, in Busan, South Korea, and has been expanded from the original presentation.

Maria Ophelia Jarligo, Georg Mauer, Martin Bram, Stefan Baumann, and **Robert Vaßen**, Institut für Energie- und Klimaforschung (IEK-1), Forschungszentrum Jülich GmbH, Jülich, Germany. Contact e-mail: m.o.jarligo@fz-juelich.de.

A good material choice for oxygen transport membranes is perovskitic lanthanum strontium iron cobalt oxide with general formula $La_{1-x}Sr_xCo_yFe_{1-y}O_{3-\delta}$ (LSCF) due to its high mixed ion-electron conductivity (MIEC) and good thermal stability (Ref 9).

Since thin films are fragile, they require one or more layers of porous support to provide integrity to the dense membrane without increasing the overall gas transport resistance at high pressure applications (Ref 10). Desirable characteristics of a good porous support for the asymmetric membrane assembly are: (i) thermal-mechanical-chemical compatibility with the membrane layer, (ii) sufficient permeability that does not dominate the permeation rate, and (iii) sufficient mechanical strength at membrane application temperature (Ref 9, 12). For manufacture using PS-PVD, a porous support that is able to withstand sintering effects during thermal spraying is an additional requirement. Metallic materials are therefore promising to meet the strict structural and process requirements of a suitable support.

Intermetallic NiCoCrAlY with high Al content (~12%) typically used as bond coat material in thermal barrier-coating (TBC) systems has been found to show good chemical compatibility with perovskite materials at high temperatures (Ref 11). Interdiffusion of elements such as Ni and Cr from the substrate that can cause negative effects on the performance of the oxygen transport membrane can be hindered by the formation of alumina scale at high temperatures which serves as diffusion barrier. NiCoCrAlY is therefore a potential material for non-shrinking porous metallic support of plasma-sprayed LSCF thin films.

First investigations of plasma-sprayed LSCF oxygen transport membrane on porous NiCoCrAlY supports have been previously reported by our group (Ref 12, 13). This work focuses on understanding the coating build-up of dense LSCF thin film on irregular surface of porous metallic support. Improved permeation rates of the membrane deposited using optimized PS-PVD process parameters as well as annealing investigations are also reported.

2. Experimental

2.1 Materials and Substrate Preparation

The LSCF feedstock material used for deposition of the membrane layer was rhombohedral perovskite with nominal composition of $La_{0.58}Sr_{0.4}Co_{0.2}Fe_{0.8}O_{3-\delta}$. Scanning electron micrograph in Fig. 1, reveals the spherical morphology of the starting powder with average particle size of 10.4 μm determined by laser scattering. The morphology of the powder feedstock was optimized such that it was fine enough to produce dense coatings but large enough to be feedable.

The porous metallic support was produced by free-sintering NiCoCrAlY powders (Sulzer Metco, Wohlen, Switzerland) with an average particle size of 24 μm in an electric furnace using 15-mm diameter by 2-mm thickness alumina mold. Figure 2 shows the cross-section of the manufactured support. Porosity was measured by image analysis of metallographic cross-sections. The mean roughness depth R_z was determined using a confocal laser microscope in accordance with the EN ISO 4287, ASME B46.1 standards.

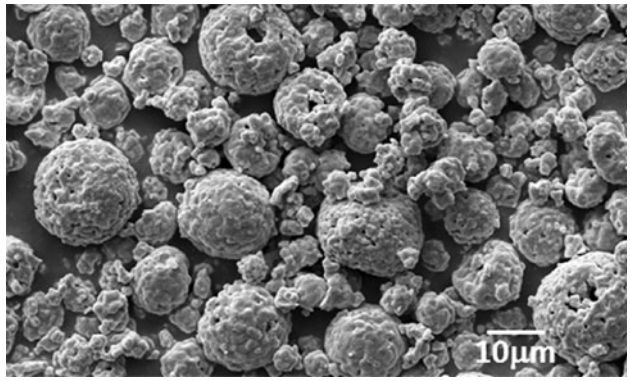

Fig. 1 Powder morphology of the LSCF feedstock

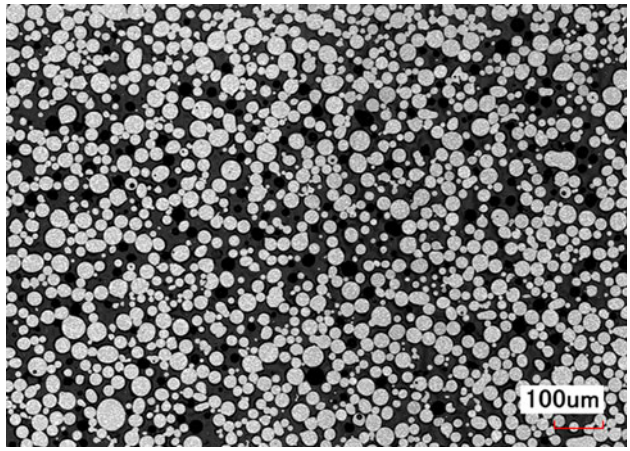

Fig. 2 Cross-section of the porous NiCoCrAlY support taken by confocal laser microscope

2.2 Membrane Layer Deposition

Coating experiments were carried-out in a PS-PVD Sulzer Metco multi-coat facility. The plasma torch used was O3CP (Sulzer Metco) with power capability of up to 150 kW and nozzle diameter of 12 mm. The torch sweep angle was set to 7°. Additional oxygen gas was fed to compensate for the reduction of LSCF during coating (Ref 10). The spray parameters used are listed in Table 1. The selected parameters were optimized from results of previous investigations (Ref 8, 12).

2.3 Membrane Characterization and O_2 Flux Measurements

Metallographic cross-sections were analyzed using a confocal laser microscope (Keyence, Germany) and a scanning electron microscope with energy dispersive

Table 1 PS-PVD parameters used to deposit LSCF thin films

Spray Parameter	Value
Chamber pressure, Pa	200
Gun current, A	2000-2400
Torch power, kW	55-57
Ar gas flow rate, slpm	100-120
He gas flow rate, slpm	15-20
Spray distance, mm	1000
Feed rate, g/min	20

slpm standard liters per minute

spectrometer (SEM-EDS) (Ultra 55, Zeiss, Germany). Thickness measurements were taken from the tip of the support to the surface of the coating. The recorded values are averages of 30 equidistant measurements along each cross-section of a sample.

Oxygen permeation measurements were carried out in a laboratory scale quartz reactor. Experimental set-up has been described elsewhere (Ref 11). Air was fed into the oxygen-rich chamber (membrane side), while argon was used as the sweep gas on the permeate (support) side. The air flow rate was 250 and 50 normal mL/min for Ar. Both gases were fed at atmospheric pressure. The temperature was monitored by a thermocouple attached close to the membrane. To minimize gas leakage, a gold ring was used to seal the membrane to the feed gas compartment. The sample was heated to 1010 °C for 4 h prior to measurement. With this condition, the gold ring was softened in order to achieve a gas-tight seal. The permeate was analyzed by online mass spectrometry. Oxygen permeation was measured at 650-1000 °C. The oxygen permeation flux was calculated as follows:

$$J_{O_2} = x(O_2)_{perm} \cdot \frac{F_{permeate}}{A_{membrane}} \quad \text{(Eq 1)}$$

where, $x(O_2)_{perm}$ is the concentration of the oxygen in the permeate, $F_{permeate}$ the volume flow rate or the permeate, and $A_{membrane}$ is the area of the membrane disc. $x(O_2)_{perm}$ was obtained by measuring the amount of leaked nitrogen from which the corresponding amount of leaked oxygen was obtained:

$$x(O_2)_{perm} = x(O_2) - x(N_2) \cdot \frac{F_{O_2-Feed}}{F_{N_2-Feed}} \quad \text{(Eq 2)}$$

where, $x(O_2)$ and $x(N_2)$ are the measured oxygen and nitrogen concentration in the permeate, respectively, and $F_{O_2-Feed}/F_{N_2-Feed}$ the ratio of the oxygen and nitrogen volume flow rate in the feed, which is approximately 0.25 in case of air.

3. Results and Discussion

Image analysis on the cross-sections of the fabricated porous MCrAlY supports revealed porosity values ranging

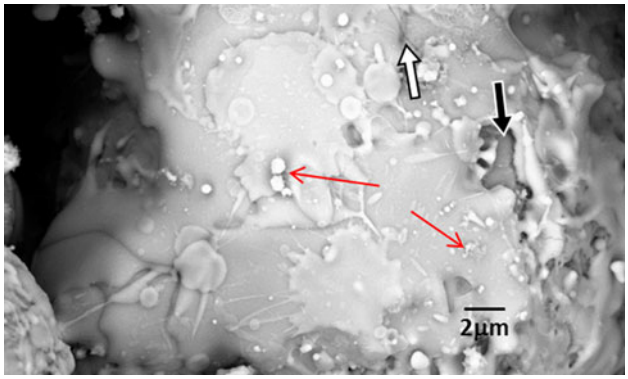

Fig. 3 Back-scattered SEM image of LSCF splats on a porous metallic NiCoCrAlY support after one spray pass

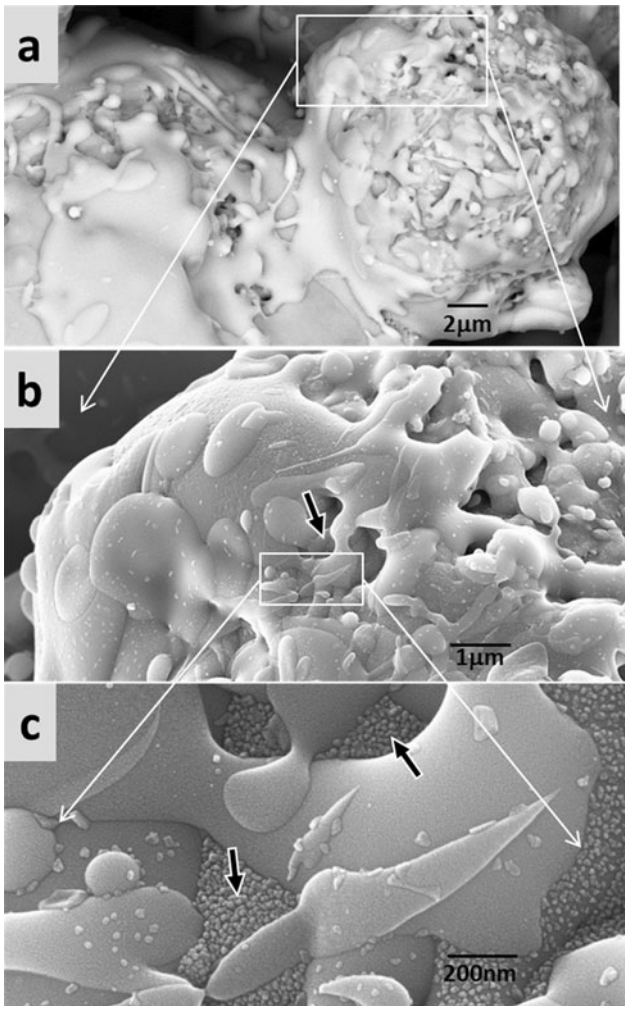

Fig. 4 Back-scattered electron images of LSCF splats on a porous metallic NiCoCrAlY support after one spray pass. The highlighted area in (a) is magnified in (b) and (c)

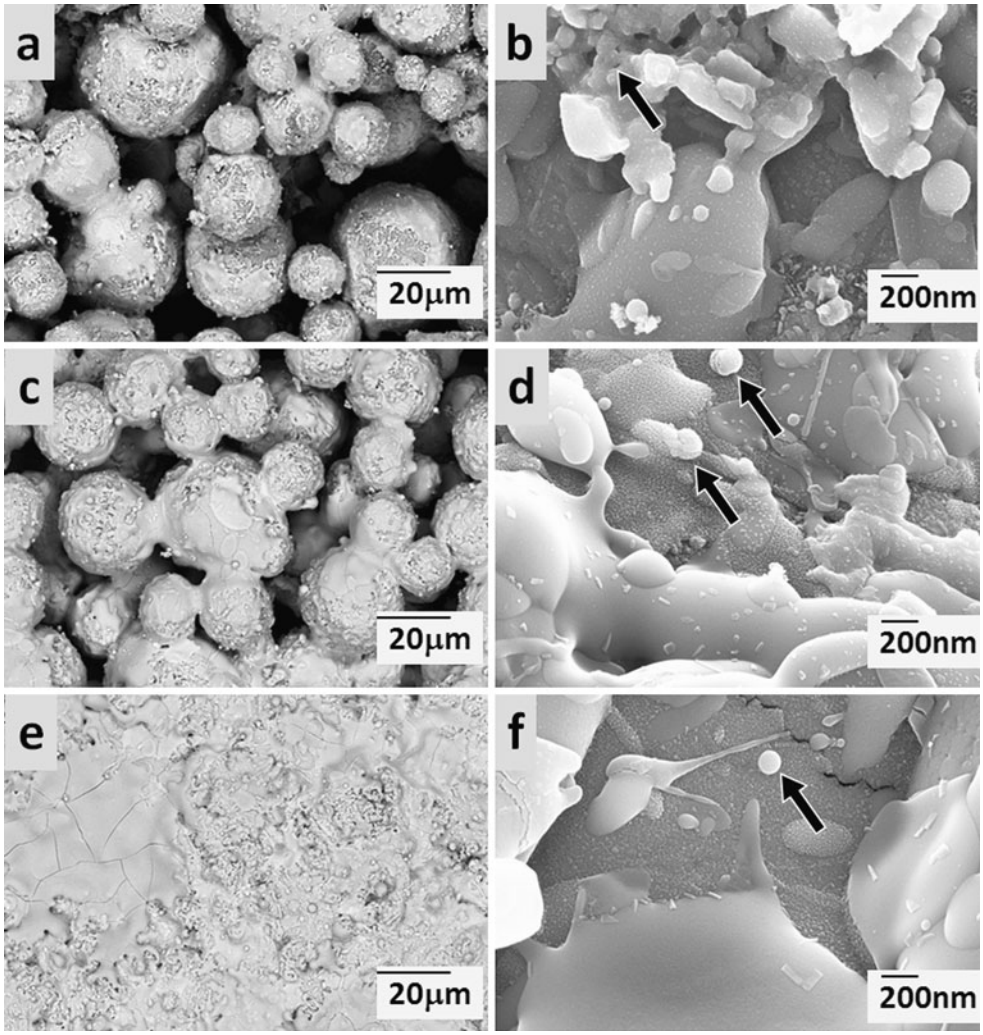

Fig. 5 Back-scattered electron images of LSCF on the surface of NiCoCrAlY particles after (a-b) 1 s, (c-d) 2 s and (e-f) 60 s of PS-PVD

from 36-42%. The average surface roughness (R_z) of the porous supports ranged from 22 to 25 μm.

3.1 Microstructure Formation and Coating Build-up

After one spray pass through the coating area which took about 1 s, overlapping splats were found to solidify from highly molten droplets that impacted the support as shown in Fig. 3. Large areas of the surficial NiCoCrAlY particles are coated with highly fluid deposits that flowed through the sides of the particles. The black arrow in the figure indicates an uncoated area, while the white arrow points to a microcrack. As the molten particle impacts the substrate, lateral microcracks typically open due to stress relaxation when the shrinkage of the solidifying splat is restricted by the massive substrate or the underlying splats during rapid cooling (Ref 14). The white nano-sized spherical particles indicated by red arrows on the surface of overlapping splats are cobalt-deficient $La_xSr_{1-x}Fe_yO$ clusters as determined by EDS. Previous study has reported that Co has higher reduction tendency than its Fe counterpart (Ref 15). In this case, the added oxygen in the spray process is not enough to prevent the partial reduction/decomposition of the LSCF. This can be prevented by increased addition of oxygen or sufficient reduction of coating temperature.

After one spray cycle, the whole surface of the spherical particles of the support are entirely covered (Fig. 4a). The crevices between the particles are also partly filled by molten droplets. These droplets have low viscosity and create a splashing effect as they hit the uneven surface of the support. The overlapping splats and splashes from multiple droplets have high tendency to leave nano-sized gaps indicated by black arrow in Fig. 4(b). When the gaps are not filled but rather covered by succeeding splats that solidify into dense lamella, they later become sealed pores in the microstructure of the deposited coatings. The gaps are also filled with several condensates tens of nanometers in size as shown in Fig. 4(c). Under PS-PVD process conditions, formation of gaseous components is typically inevitable as the plasma core temperature reaches several thousand Kelvin higher than the melting temperature of the feedstock

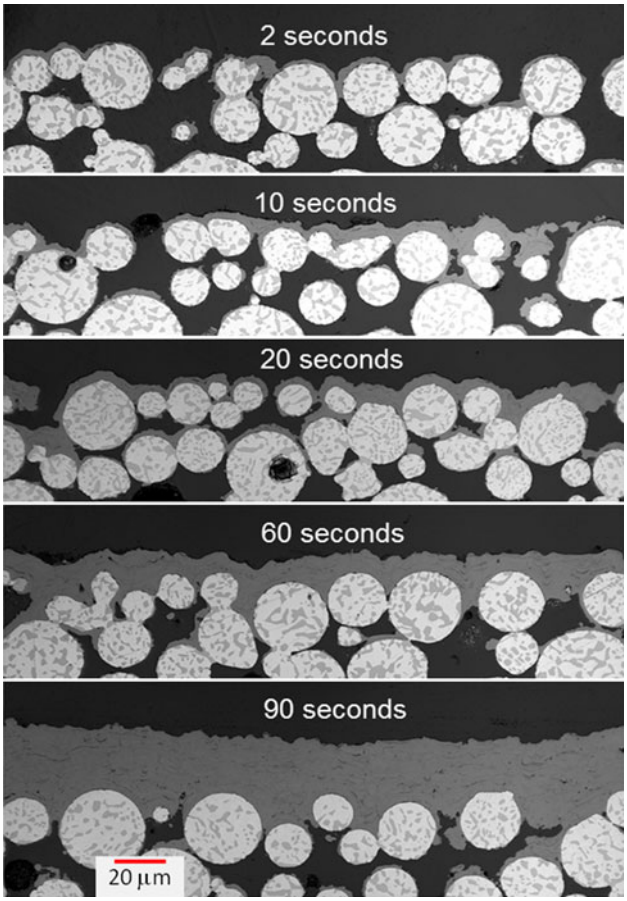

Fig. 6 Cross-section images by confocal laser microscope of LSCF coatings on porous NiCoCrAlY supports after several coating times

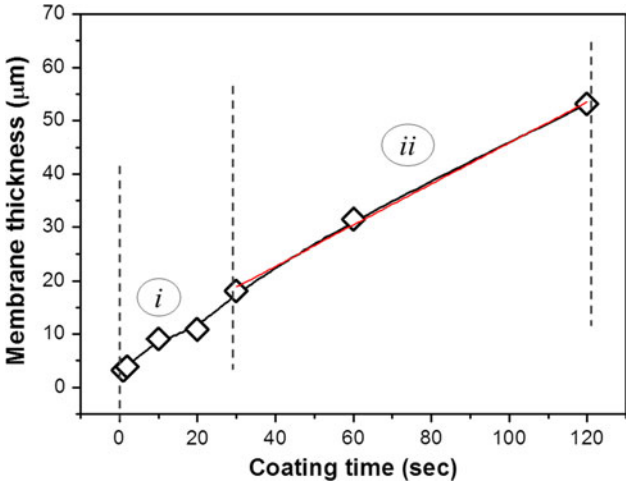

Fig. 7 Membrane thickness on porous NiCoCrAlY supports as a function of coating deposition time

material (Ref 8). Nano-sized condensates found on the surface of highly molten splats solidify due to the sudden change in temperature near the surface of the underlying splat as the plasma plume moves away from the target. They

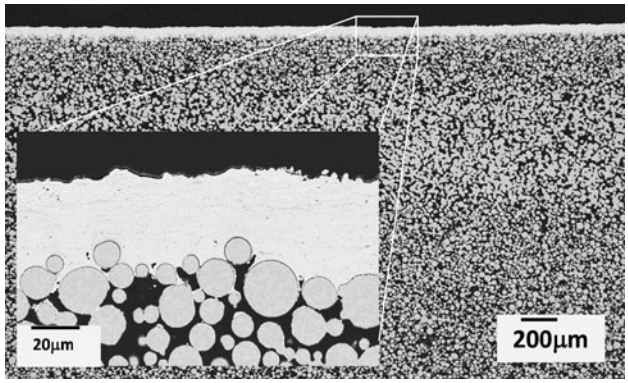

Fig. 8 Cross-section of the asymmetric oxygen transport membrane after 120 s of LSCF deposition by PS-PVD

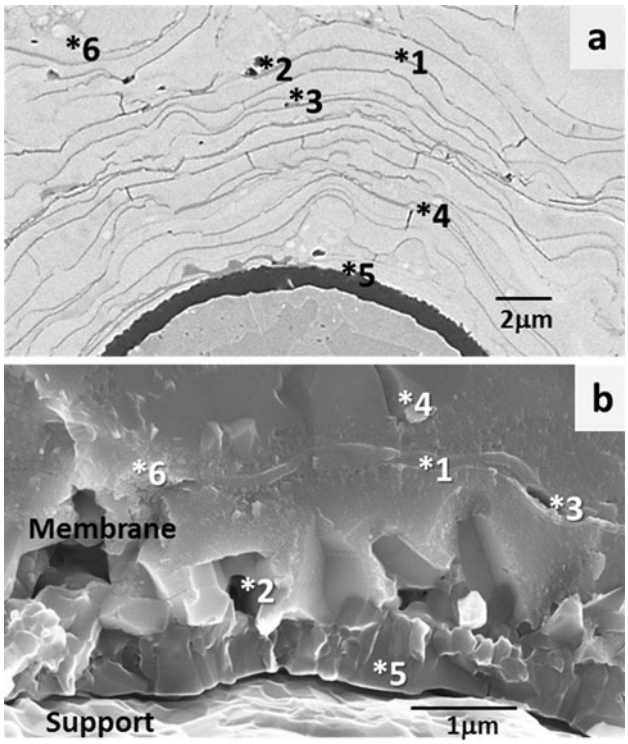

Fig. 9 SEM image of a (a) polished and (b) fractured cross-section, showing the microstructural features of LSCF membrane deposited by PS-PVD on porous NiCoCrAlY support

are eventually covered by overlapping molten deposits and become an integral component of the nano-sized splat formation in the dense coating. As the plasma plume oscillates, the surface of the target is kept thermodynamically active allowing for extended flowability of the liquid splats. The recorded surface temperature ranged from 800 to 1000 °C. When the coating builds up, the underlying splats become more viscous probably due to increasing temperature gradient through the coating.

Back-scattered electron surface images of LSCF coatings as they build-up on the porous metallic support after several deposition times are shown in Fig. 5(a)-(f). After two seconds, the spherical particles of the support are still

recognizable (Fig. 5a, c). Formation of clusters indicated by a black arrow in Fig. 5(b) can be observed. These clusters could have formed from the re-solidification and agglomeration of nano-condensates or molten droplets as indicated by black arrows in Fig. 5(d) and (f). Previous study has reported that these clusters are believed to have been formed from incomplete vaporization or nucleation and growth (Ref 16). After coating for 60 s, the spherical particles of the support are no longer visible and the inter-particle gaps are filled. However, the surface of the coating still exhibits significant roughness and microcracks.

Cross-section images in Fig. 6 show another perspective of the coating build-up on porous metallic support. The initial coating stage which corresponds to (i) in Fig. 7, is primarily filling up of crevices between spherical particles of the support. As observed in the cross-sections, sub-layers of the support are also coated with LSCF. Molten droplets go through the open gaps between surficial particles and deposit on the sub-layers. The solidified lamellae take on the form of the particle surface. If the gaps between spherical particles on the surface and the sub-layer are wide, the solidified dense coating also forms deep valleys with large pores or cracks. Based on the evolution of coating microstructures, it is therefore desirable to keep the R_z value as low as possible to avoid higher chances of producing microstructural defects during coating. Stage (i) takes approximately 30 s for an average support roughness R_z of ~25 μm. The thickness of the deposited coating is also not far from this value. This means, that R_z values can be used to estimate the coating thickness that is needed to fill the surficial gaps between spherical particles until a relatively planar thin film deposit starts to form (ii). The complete asymmetric oxygen transport membrane assembly is shown in Fig. 8. The LSCF thin film has a thickness of about 55 μm after coating for 120 s. Inset image reveals the homogeneous dense thin film deposit on a highly irregular surface of the porous metallic support. The fabricated membrane was gastight after air leak test through vacuum suction.

Figure 9 shows the interface region between the membrane layer and the porous support. The polished cross-section in Fig. 9(a) shows a good bonding between the support and the membrane. Different microstructures comprising (1) lamellar interface, (2) micropores, (3) nanopores, (4) vertical microcracks, (5) alumina scale, and (6) clusters were formed. Vertical microcracks result from stress release when the substrate or underlying splat temperature changes as the coating deposition progresses. Corresponding numbered microstructural features can also be observed in a fractured cross-section in Fig. 9(b). It can be observed that nano-splats build-up the dense coating lamella. In addition, in-situ formation of the desired alumina diffusion barrier has been achieved. The thickness of the reaction zone is in the nano-range which has to be considered for application. The impact of interdiffusion (Al into the perovskite membrane and Sr consumption for oxide formation) on the permeation rate of the membrane system should be insignificant (Ref 11).

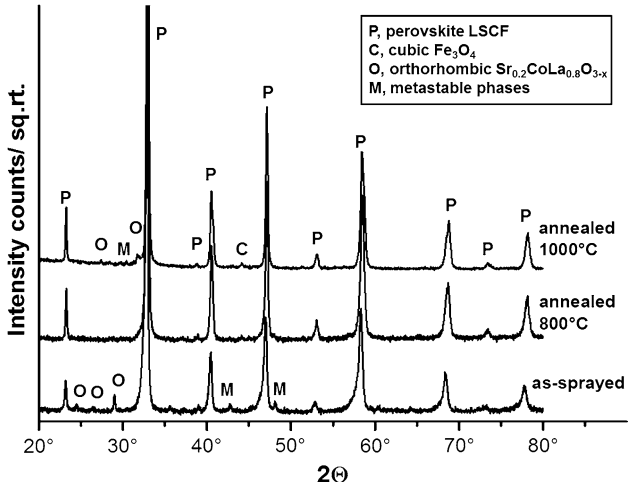

Fig. 10 X-ray diffraction profiles of LSCF deposited by PS-PVD

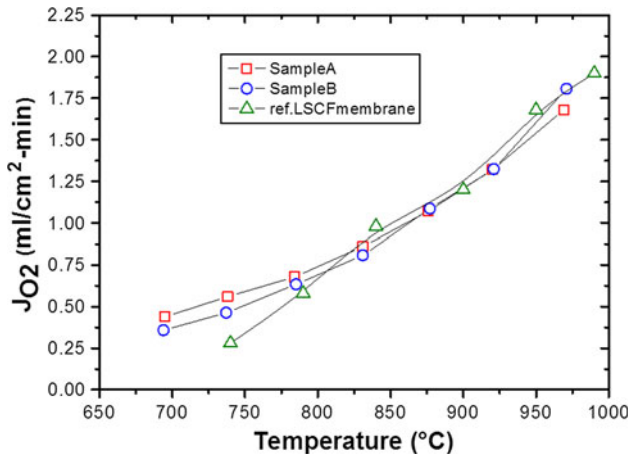

Fig. 11 Measured oxygen flux through the LSCF membrane deposited by PS-PVD on NiCoCrAlY support

3.2 Phase Stability of the LSCF Membrane

X-ray diffraction analysis (Fig. 10) reveals that the as-sprayed thin films consist of perovskite LSCF higher than 95%. Minor content of orthorhombic $Sr_{0.2}CoLa_{0.8}O_{3-x}$ and metastable oxide phases containing Co and Fe were also observed. After annealing in air for 2 h at 800 °C, LSCF remained perovskite and the intensities of the metastable phases decreased. Further annealing at 1000 °C increased the crystallinity of the perovskite phase and the reflections of the secondary oxides became insignificant except for orthorhombic $Sr_{0.2}CoLa_{0.8}O_{3-x}$ and cubic Fe_3O_4, which became more pronounced.

3.3 Oxygen Transport Properties

Oxygen permeation flux results of the fabricated asymmetric membranes using LSCF by PS-PVD on NiCoCrAlY supports (Samples A and B) are shown in Fig. 11. The measured values were obtained after 3 h at each

temperature step in steady-state condition. Minor gas leaks were recorded and subtracted from the raw values of the oxygen permeation rates using Eq 2. Gas leak might be due to the presence of microcracks and nano-pores in the membranes, and could also originate from insufficient sealing of the gold ring. Permeation rates were obtained without any flux enhancement or activation procedures, and are very close to reported best performing conventionally prepared LSCF oxygen transport membrane of similar thickness (Ref 17). These results are more than three times higher compared to our previously reported values in (Ref 12). This is probably due to the deposition of higher percentage of perovskite phase using the optimized spray parameters.

4. Conclusions

Deposition of small and highly flow able splats as well as clusters and nano-condensates by PS-PVD, build-up into thin and dense LSCF coatings on porous and metallic NiCoCrAlY supports. Moreover, the surface roughness of the support influences the coating build-up. The PS-PVD process has the advantage of in-situ formation of thin alumina interdiffusion protection layer, hence additional sintering process typically employed in wet chemical routes of depositing LSCF thin films is no longer required. Optimization of spray parameters was able to deposit more homogeneous coatings with higher percentage of perovskite phase in the as-sprayed coating that remains stable after annealing up to 1000 °C. The oxygen permeation results of the manufactured LSCF thin films show more improved values from 700 to 950 °C. Therefore, high quality and cost effective oxygen transport membranes for high temperature application can be achieved by the deposition of dense LSCF thin films on porous metallic supports by PS-PVD. The permeation rates can still be improved by further reduction of membrane thickness and incorporation of catalytic active porous top- and inter-layers.

Acknowledgement

The support of IEK-1, Forschungszentrum Jülich GmbH colleagues, Mr. Ralf Laufs in coating deposition, Mr. Mark Kappertz for metallographic preparations and Dr. Doris Sebold in obtaining SEM images are highly acknowledged. The research leading to these results has received funding from the European Community's Seventh Framework Programme (FP7/2007-2013) under grant agreement no. 241309 (Project acronym: DEMOYS).

References

1. K. von Niessen, M. Gindrat, and A. Refke, Vapor Phase Deposition Using Plasma Spray—PVD, *J. Therm. Spray Technol.*, 2010, **19**(1-2), p 502-509
2. A. Hospach, G. Mauer, R. Vaßen, and D. Stöver, Characteristics of Ceramic Coatings Made by Thin Film Low Pressure Plasma Spraying (LPPS-TF), *J. Therm. Spray Technol.*, 2012, **21**(3-4), p 435-440
3. B.J. Harder, and D. Zhu, Plasma Spray-Physical Vapor Deposition (PS-PVD) of Ceramics for Protective Coatings, *Advanced Ceramic Coatings and Materials for Extreme Environments: Ceramic Engineering and Science Proceedings*, Vol 32, D. Zhu, H.-T. Lin, Y. Zhou, S. Widjaja, D. Singh, Eds., Wiley, Hoboken, 2011, p 71-84
4. K. von Niessen and M. Gindrat, Plasma Spray-PVD: A New Thermal Spray Process to Deposit Out of the Vapor Phase, *J. Therm. Spray Technol.*, 2011, **20**(4), p 736-743
5. A. Refke, M. Gindrat, K. v. Niessen, and R. Damani, LPPS Thin Film: A Hybrid Coating Technology Between Thermal Spray and PVD for Functional Thin Coatings and Large Area Applications, *Thermal Spray 2007: Global Coating Solutions*, on CD-ROM, B.R. Marple, M.M. Hyland, Y.-C. Lau, C.-J. Li, R.S. Lima, and G. Montavon, Eds., May 14-16, 2007, Beijing, ASM International, Materials Park, 2007, p 705-710
6. S. Baumann, J.M. Serra, M.P. Lobera, S. Escolástico, F. Schulze-Küppers, and W.A. Meulenberg, Ultrahigh Oxygen Permeation Flux through Supported $Ba_{0.5}Sr_{0.5}Co_{0.8}Fe_{0.2}O_{3-\delta}$ Membranes, *J. Membr. Sci.*, 2011, **377**, p 198-205
7. M. Gindrat and R. Damani, LPPS Hybrid Technologies for Emerging Energy Applications—Recent Developments, *International Thermal Spray Conference*, 27-30 September 2011, Hamburg, 2011
8. G. Mauer, A. Hospach, and R. Vaßen, Process Development and Coating Characteristics of Plasma Spray-PVD, *Surf. Coat. Technol.*, 2013, **220**, p 219-224
9. O. Büchler, J.M. Serra, W.A. Meulenberg, D. Sebold, and H.P. Buchkremer, Preparation and Properties of Thin LSFC Perovskitic Membranes Supported on Tailored Ceramic Substrates, *Solid State Ion.*, 2007, **178**, p 91-99
10. J.R. McCutcheon and M. Elimelech, Influence of Membrane Support Layer Hydrophobicity on Water Flux in Osmotically Driven Membrane Processes, *J. Membr. Sci.*, 2008, **318**, p 458-466
11. Y. Xing, S. Baumann, D. Sebold, M. Rüttinger, A. Venskutonis, W.A. Meulenberg, and D. Stöver, Chemical Compatibility Investigation of Thin-Film Oxygen Transport Membranes on Metallic Substrates, *J. Am. Ceram. Soc.*, 2011, **94**(3), p 861-866
12. N. Zotov, A. Hospach, G. Mauer, D. Sebold, and R. Vaßen, Deposition of $La_{1-x}Sr_xFe_{1-y}Co_yO_{3-\delta}$ Coatings with Different Phase Compositions and Microstructures by Low-Pressure Plasma Spraying-Thin Film (LPPS-TF) Processes, *J. Therm. Spray Technol.*, 2012, **21**(3-4), p 441-447
13. N. Zotov, S. Baumann, W.A. Meulenberg, and R. Vaßen, La-Sr-Fe-Co Oxygen Transport Membranes on Metal Supports Deposited by Low Pressure Plasma Spraying-Physical Vapour Deposition, *J. Membr. Sci.*, 2013, **442**, p 119-123
14. S. Sampath, U. Schulz, M.O. Jarligo, S. Kuroda, *MRS Bulletin: Thermal-Barrier Coatings for more Efficient Gas-Turbine Engines, Processing Science of Advanced Thermal-Barrier Systems*, Vol 37(10), D.R. Clarke, M. Oechsner, N.P. Padture, Ed., October 2012, p 903-910
15. F.J. Berry, J.F. Marco, and X. Ren, Reduction Properties of Phases in the System $La_{0.5}Sr_{0.5}MO_3$ (M = Fe, Co), *J. Solid State Chem.*, 2005, **178**(4), p 961-969
16. G. Mauer and R. Vaßen, Plasma Spray-PVD: Plasma Characteristics and Impact on Coating Properties, 12th High-Tech Plasma Processes Conference (HTPP-12), *J. Phys. Conf. Ser.*, 2012, **406**, p 012005
17. W.A. Meulenberg, S. Baumann, W. Schafbauer, F. Schulze-Küppers, H.P. Buchkremer, *Stable High-Performance Oxygen Transport Membranes*, International Conference on Inorganic Membranes, Enschede, 10-13 July, 2012